

## **Supplementary Information**

# **Glass and Bioglass Nanopowders by Flame Synthesis**

Tobias J. Brunner, Robert N. Grass, Wendelin J. Stark\*

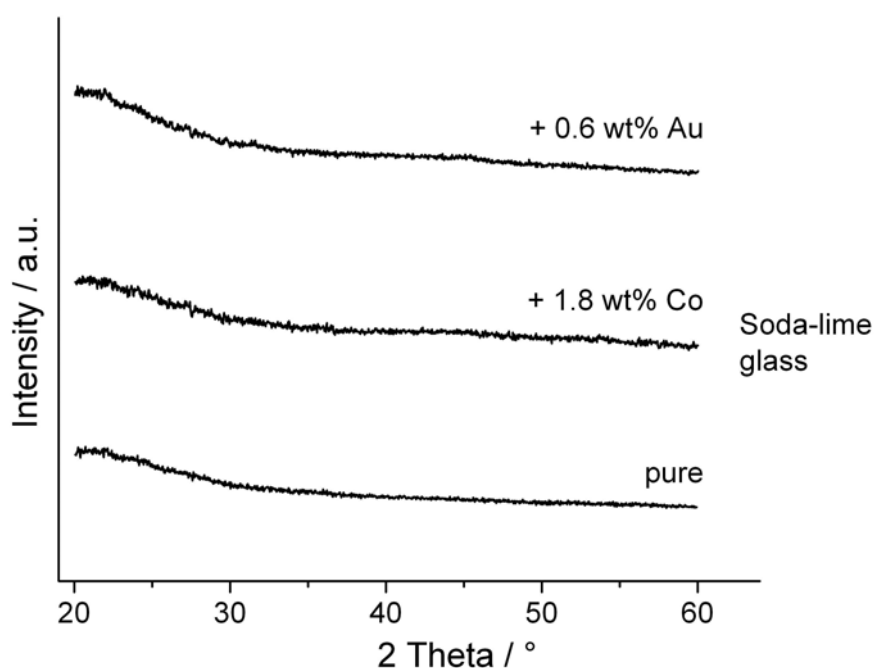
Institute for Chemical and Bioengineering, Department of Chemistry and Applied Biosciences, ETH  
Zurich, 8093 Zurich, Switzerland

\* Wendelin J. Stark  
Institute for Chemical and Bioengineering, HCI E 107  
ETH Hoenggerberg  
Wolfgang-Pauli-Str. 10  
CH-8093 Zurich  
Switzerland

e-mail: [wendelin.stark@chem.ethz.ch](mailto:wendelin.stark@chem.ethz.ch)  
phone: +41 44 632 09 80  
fax: +41 44 633 10 83

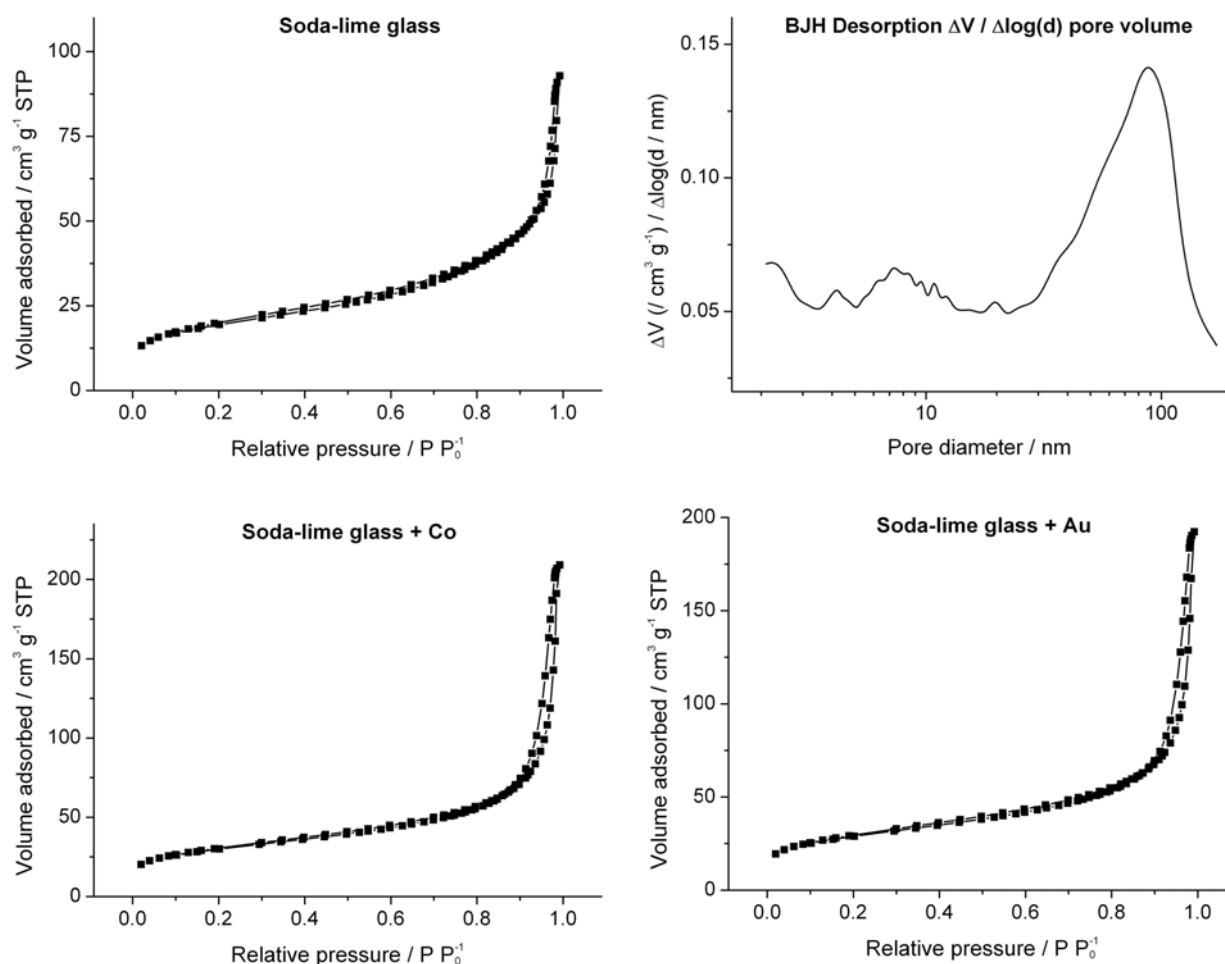
## Influence of cobalt and gold doping

In order to illustrate that the addition of 0.6 wt% gold or 1.8 wt % cobalt did not significantly affect the formation of amorphous soda-lime glass during flame synthesis, the corresponding X-ray diffraction (XRD) pattern are compared within Fig. S1.



**Fig. S1** X-ray diffraction pattern of soda-lime glass, pure (bottom trace), doped with 1.8 wt% cobalt (2<sup>nd</sup> trace) and doped with 0.6 wt% gold (top trace).

Since both doped and pure soda-lime glasses did not show any changes in the XRD pattern, it may be concluded that the dopants did not induce the formation of separate crystalline phases. The low content of gold and the size of the particles (top trace) are too small to provoke measurable reflections in the XRD. This is consistent with observations of gold on silica or titania at similar gold content (0.5 wt%)<sup>1</sup>.

**Nitrogen adsorption isotherms of as-prepared glasses**

**Fig. S2** Adsorption-desorption isotherm plots for soda-lime glass (top left), soda-lime glass doped with cobalt (bottom left) and gold (bottom right). For pure soda-lime glass the pore size distribution of the desorption branch is shown at the top right.

Nitrogen adsorption was performed at liquid-nitrogen temperature with a Micromeritics TriStar 3000 apparatus measuring 86 points. Prior to the measurements the samples were degassed at 150°C for 1h. The Barrett-Joyner-Halendar (BJH) method was applied to evaluate the adsorbed volumes and pore size distributions.

### Oxidation state of gold and cobalt dopants in soda-lime glass

The oxidation state of gold on an oxidic surface after material preparation in a similar high-temperature environment has been investigated by Mädler et al.<sup>1</sup> for gold on pure silica or titania. UV-VIS spectroscopy revealed the presence of zero-valent, metallic gold nanoparticles which gave rise to plasmon-type absorption pattern in the UV-VIS spectra in the range of 450 to 600 nm<sup>1</sup>.

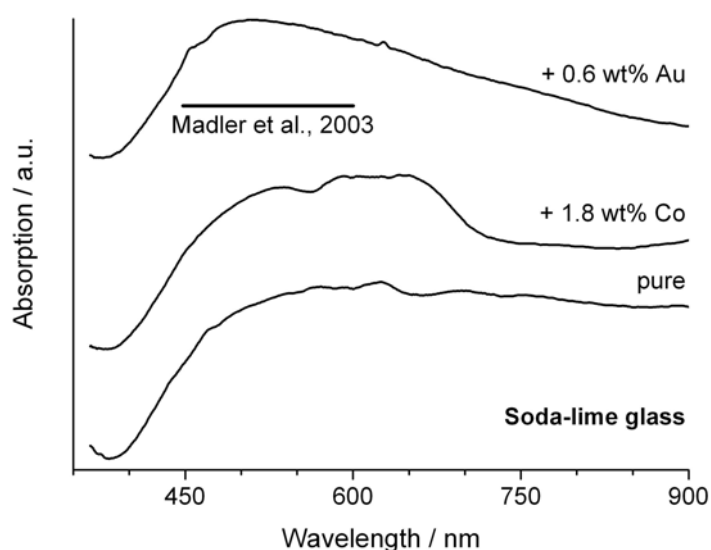


**Fig. S3** UV-VIS spectra of soda-lime glass, pure (bottom), with cobalt (II) or metallic gold incorporated into the glass matrix.

Figure S3 compares pure soda-lime glass with samples containing 0.6 wt% gold or 1.8 wt% cobalt. The UV-VIS spectrum of pure soda-lime glass does not show any pronounced features in agreement with a lack of suitable chromophores in this silicate. The shoulder starting at around 500 nm can be attributed to the influence of scattering as shown by Grass et al.<sup>2</sup> Addition of cobalt resulted in two broad, ill-defined signals observed around 500 and 650 nm with low intensity. These absorptions can be attributed

to d-d transitions of ionic cobalt. The addition of gold gives rise to the previously described plasmon-type absorptions around 500 nm<sup>1</sup>.

The UV-VIS spectra were recorded on a Shimadzu UV-1650PC spectrophotometer using a specular reflectance measurement attachment.

## Particle homogeneity and element distribution

The high homogeneity of mixed oxides prepared from suitable precursors in flame synthesis has been investigated previously for vanadia/titania<sup>3</sup>, titania doped silica<sup>4</sup> and ceria/zirconia solid solutions<sup>5,6</sup>. Mixed oxides containing three different metals as a mixture have been prepared by Schulz et al.<sup>7</sup>. These previous investigations repeatedly showed that highly consistent compositions could be achieved even on the level of different particles<sup>3-6</sup>. The high homogeneity of the present material therefore stays in agreement with these earlier investigations.

The chemical homogeneity was further supported by laser ablation inductively coupled plasma mass spectrometry (LA-ICP-MS, Table S1 and S2).

**Table S1** ICP-MS results for soda-lime glass doped with gold

| Run number     | Ca/Si (wt%)  | Na/Si (wt%)  | Au/Si (wt%)    |
|----------------|--------------|--------------|----------------|
| Run 1          | 0.212        | 0.294        | 0.01231        |
| Run 2          | 0.214        | 0.306        | 0.01283        |
| Run 3          | 0.204        | 0.277        | 0.01234        |
| Run 4          | 0.211        | 0.298        | 0.01234        |
| Run 5          | 0.213        | 0.299        | 0.01271        |
| Run 6          | 0.214        | 0.285        | 0.01254        |
| Run 7          | 0.213        | 0.273        | 0.01266        |
| Run 8          | 0.211        | 0.275        | 0.01251        |
| <b>Average</b> | <b>0.212</b> | <b>0.288</b> | <b>0.01253</b> |
| St. dev.       | 0.003        | 0.013        | 0.00019        |

**Table S2** ICP-MS results for Bioglass 45S5

| Run number     | Ca/Si (wt%)  | Na/Si (wt%)  | P/Si (wt%)   |
|----------------|--------------|--------------|--------------|
| Run 1          | 0.780        | 0.724        | 0.089        |
| Run 2          | 0.786        | 0.746        | 0.087        |
| Run 3          | 0.780        | 0.753        | 0.090        |
| Run 4          | 0.801        | 0.736        | 0.089        |
| Run 5          | 0.816        | 0.745        | 0.089        |
| Run 6          | 0.812        | 0.777        | 0.091        |
| Run 7          | 0.819        | 0.765        | 0.092        |
| Run 8          | 0.823        | 0.756        | 0.091        |
| <b>Average</b> | <b>0.802</b> | <b>0.750</b> | <b>0.090</b> |
| St. dev.       | 0.018        | 0.017        | 0.002        |

**Laser-ablation ICP-MS.** The glass analyses were carried out using an 193 nm ArF excimer laser ablation system (Lambda Physik, Göttingen Germany) coupled to an ICP-MS (DRC II +, Perkin Elmer, Norwalk, USA)<sup>8</sup>. The samples were ablated for 60 s (10Hz, 60 and 80  $\mu$ m crater diameter) and the results summarized in Tables S1 and S2. The reference material NIST 610 was used as external calibration standard. Data reduction and concentration calculation was carried out using the protocol as described by Longerich et. al.<sup>9</sup>.

### Morphology of as-prepared bioglass nanoparticles

Transmission electron microscopy of as-prepared bioglass (Fig. 1) corroborated that the material consisted of 20-50 nm sized nanoparticles. In order to provide an overview of the material, a scanning electron microscopy image of as prepared and sintered bioglass 45S5 is compared within Figure S4 at the same magnification. While the nanoparticles are barely visible (Fig. S4, left), sintering resulted in much larger features and agglomerated and partially sintered particles of up to several hundred nanometers (Fig. 4S, right).

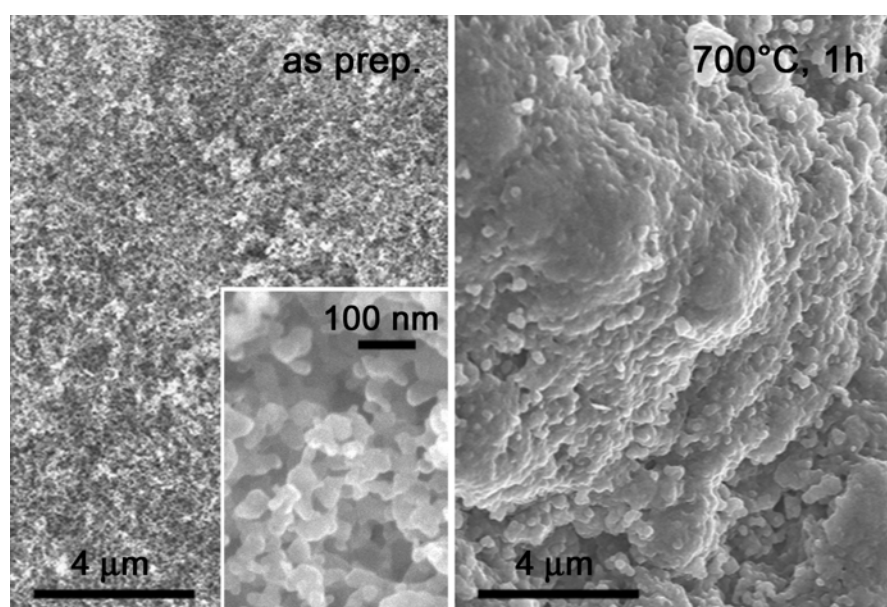


**Fig. S4** Scanning electron microscopic image of as-synthesized Bioglass 45S5 (left) displaying the high homogeneity of the material. The inset shows a higher magnification of untreated bioglass. After calcination at 700°C for 1 hour (right) the material is vigorously sintered.

A TEM image of Co-doped soda-lime glass is depicted in Fig. S5. This nanopowder also consists of regular, partially agglomerated, mainly spherical particles with no evidence for crystallites or phase segregation (comparable to Bioglass 45S5, see Fig. 1) which further confirms the results on particle homogeneity.



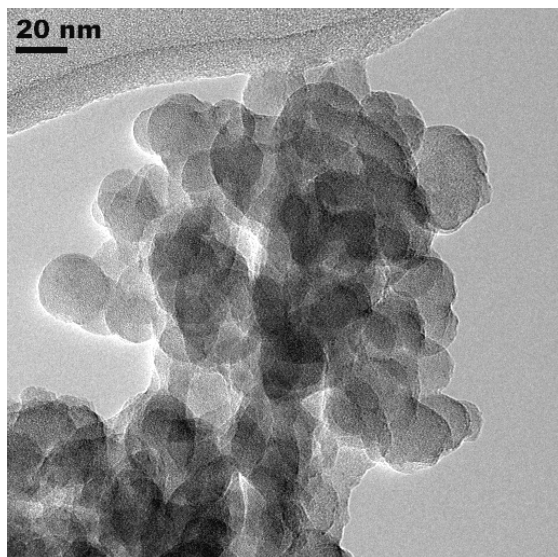


Fig. S5 Transmission electron microscopic image of soda-lime glass doped with cobalt.

## References

- 1 L. Madler, W.J. Stark, and S.E. Pratsinis, *J. Mater. Res.*, 2003, **18**, 115-20.
- 2 R.N. Grass and W.J. Stark, *Chem. Commun.*, 2005, 1767-9.
- 3 W.J. Stark, K. Wegner, S.E. Pratsinis, and A. Baiker, *J. Catal.*, 2001, **197**, 182-91.
- 4 W.J. Stark, S.E. Pratsinis, and A. Baiker, *J. Catal.*, 2001, **203**, 516-24.
- 5 W.J. Stark, L. Madler, M. Maciejewski, S.E. Pratsinis, and A. Baiker, *Chem. Commun.*, 2003, 588-9.
- 6 W.J. Stark, M. Maciejewski, L. Madler, S.E. Pratsinis, and A. Baiker, *J. Catal.*, 2003, **220**, 35-43.
- 7 H. Schulz, W.J. Stark, M. Maciejewski, S.E. Pratsinis, and A. Baiker, *J. Mater. Chem.*, 2003, **13**, 2979-84.
- 8 F. Ottinger, I. Kroslakova, K. Hametner, E. Reusser, R. Nesper, and D. Gunther, *Anal. Bioanal. Chem.*, 2005, **383**, 489-99.
- 9 H.P. Longerich, S.E. Jackson, and D. Gunther, *J. Anal. Atom. Spectr.*, 1996, **11**, 899-904.